RSC Advances

ROYAL SOCIETY OF CHEMISTRY

www.rsc.org/advances

Cite this: DOI: 10.1039/c0xx00000x

www.rsc.org/xxxxxx

ARTICLE TYPE

Comparison of Nonlinear Optical Chromophores Containing Different Conjugated Electron-bridges: the Relationship between Molecular Structure-properties and Macroscopic Electro-optic Activities of Materials

Jieyun Wu,[a*] Hongyan Xiao,[b] Ling Qiu,[b] Zhen Zhen,[b] Xinhou Liu,[b] and Shuhui Bo[b*]

Received (in XXX, XXX) Xth XXXXXXXXX 20XX, Accepted Xth XXXXXXXXX 20XX
DOI: 10.1039/b000000x

In electro-optic（EO） materials, realization of large EO coefficients for organic EO materials requires the simultaneous optimization of chromophore first hyperpolarizability, acentric order, molecular shape et al. As these parameters are complicatedly inter-related, thorough analyses are required to understand the dependence of macroscopic EO activity upon chromophore structure and property. Herein, we represented the synthesis of three chromophores containing different conjugated electron-bridges by acidic and alkaline formylation. Electron-rich moieties thiophene and formyl-thiphene in the different positions of chromophores played the different roles of electron-bridge, site-isolator and electron-isolator, generating the intrigued property variations of electron-distribution of push-pull structure, intramolecular charge-transfer, solvatochromism, microscopic hyperpolarizability and related density functional theory calculation results. And those molecular structure-property relationships were rationally related to the EO activities to understand the impact of microscopic molecular property on macroscopic EO activities of materials.

1. Introduction

The organic nonlinear optical (NLO) chromophores, which possessed the push-pull structure of donor-conjugated electron bridge-acceptor (D-π-A), have been widely reported as the promising materials for the photonic devices. Peculiarly, the research of organic and polymeric electro-optic (EO) materials based on second order NLO chromophores has made tremendous progress.[1-4] Microscopically, the nonlinearity of chromophores was represented as the hyperpolarizability (β) and the dipole moment (μ). For the real application, it required the macroscopic nonlinearity (EO coefficients: r_{33}) of materials and devices. Hence, NLO chromophores were incorporated into either the host polymer matrix, or by covalently attaching them into a suitable polymer substrate. Electrical field induced poling was applied to induce the acentric ordering of chromophores in polymers, which translated microscopic hyperpolarizability of chromophores into macroscopic EO coefficients of materials. Significant advances in the development of new-generation organic EO materials have been made through rational chromohore design, which has led to a successful demonstration of ultrahigh EO coefficients.[5-7]

The design and synthesis of the NLO chromophores with large μ and β have been achieved. However, how to efficiently translate the molecular microscopic β value into macroscopic EO activities of materials was a confused problem. In electrical induced poling, it was easy to induce dipole-dipole interactions of chromophores with large $\mu\beta$ values. Those dipole-dipole interactions generated the antiparallel packing of chromophores to form the dimers, reducing the efficiency of translating the microscopic hyperpolarizability of chromophores into macroscopic EO coefficients in materials. To attenuate the dipole-dipole interaction, Larry Dalton and Alex K-Y Jen proposed the strategy of site-isolation, which was supposed to distance the neighbor chromophores in EO polymers.[3,8-10] In this respect, the translation efficiency of molecular microscopic β value into macroscopic EO coefficients was significantly improved.[5,10,11] Based on the above work, Li Zhen proposed the concept of suitable isolation group and testified that introduction of suitable steric hindrance group could effectively attenuate the dipole-dipole interactions and improved the EO coefficients.[12-17] Series of chromophores containing suitable isolation such as pentafluorobenzene, dendritic group showed promising nonlinearity.[13,18-27]

In our recent research, diene-bridge based chromophore **WJ1** (scheme. 1) containing site-isolator thiophene perpendicular to the conjugated plane showed ultrahigh EO coefficients (337 pm/V) in guest-host EO materials.[28] Zhang ML et al synthesized a diene-bridge based chromophore **B** (scheme. 1) but achieved rather different EO activities in guest-host EO materials.[29] Herein, as a follow-up research, this article presented the synthesis and property variation of three chromophores **WJ1**, **WJ2** and **WJ9** (scheme. 1) containing different conjugated electron-bridges. Comparing with conventional divinylthiophene-bridge based **WJ9**, chromophores **WJ1** and **WJ2** containing site-

isolators thiophene and formyl-thiophene showed the much different properties of intramolecular charge-transfer, solvatochromism, microscopic nonlinearity and related DFT calculation results. More intriguingly, thiophene and formyl-thiophene perpendicular to the conjugated plane of **WJ1** and **WJ2** was found to have the different degree of electron-isolation function, which helped to attenuate the dipole-dipole interactions of chromophores and to achieve the high EO coefficients in guest-host EO polymeric materials even at high chromophore loading density.

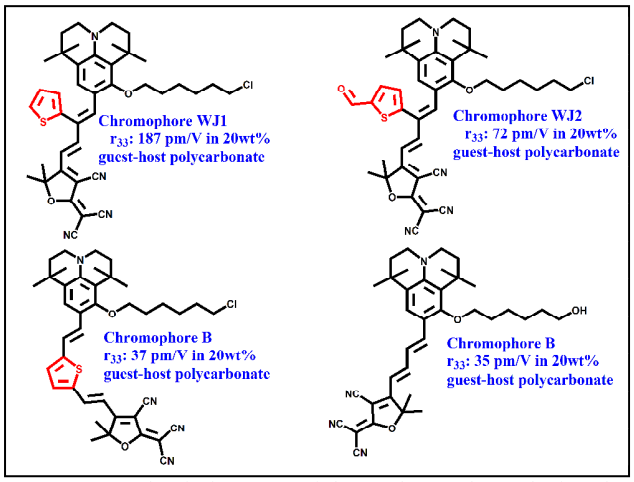

Scheme. 1 Chemical structure of chromophores. The synthesis and related data of chromophore **B** can be found in reference 29.

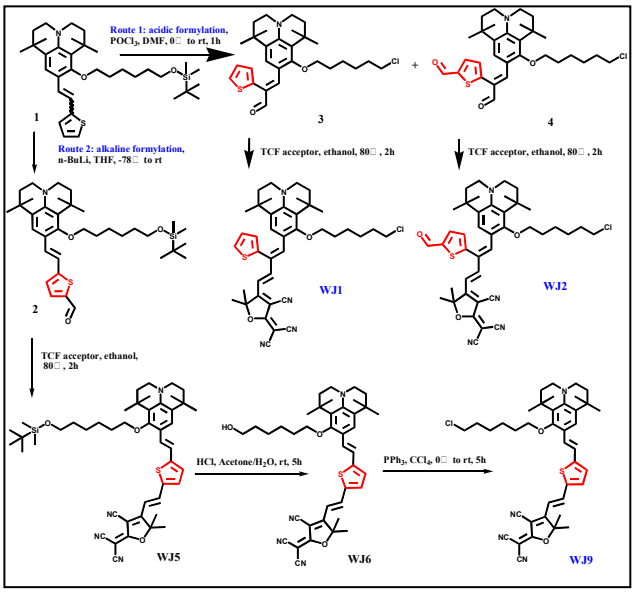

Scheme 2. Synthesis of Chromophores

2. Results and discussions

2.1 Synthesis and Structure Analysis

Scheme 2 showed the synthetic route of chromophores **WJ1**, **WJ2** and **WJ9.** The formylation of donor-bridge compound **1** was preceded under acidic and alkaline conditions respectively to prepare different donor-bridges **2**, **3** and **4**. In acidic Vilsmeier reaction, the intramolecular H-bond interaction and cis-trans isomerism changed the electron distribution of compound **1**.[28] Formylation of compound **1** reacted at carbon-carbon double bond preferentially. Meanwhile, the deprotection of hydroxy group and halogenation were proceeded to form compound **3**. Feeding excessive phosphorus oxychloride ($POCl_3$), formylation then reacted on the ortho-position of thiophene to facilitate compound **4**. **Table 1** demonstrated the feed ratio of $POCl_3$ and compound **1**, as well as the yield of products **3** and **4**. When less than 1 equivalent (eq) $POCl_3$ reacted with compound **1**, it only produced compound **3**. As the molar ratio of $POCl_3$ and compound **1** raised to 2:1, the products were facilitated as the mixed compounds of **3** and **4**. This result inferred that Vilsmeier formylation primarily reacted on the double bond and secondly reacted on the ortho-position of thiophene. Increased equivalent of $POCl_3$ (>2eq) resulted in the higher yield of compound **4** and the lower yield of **3**. However, the overall yield of compounds **3** and **4** was reduced, which inferred that excessive $POCl_3$ was not beneficial for the formylation. In alkaline formylation, compound **1** was formylated with *n*-butyl lithium and DMF to form compound **2**. After the Knoevenagel condensation of compounds **3**, **4** and tricyanofuran acceptor (TCF), chromophores **WJ1** and **WJ2** were obtained with the yield of 72% and 46 %, respectively. The additional electron-withdrawing formyl group on thiophene made the electron density of compound **4** lower than **3**, which might be the reason that the yield of **WJ2** was lower than **WJ1**. In order to synthesize chromophore **WJ9** containing the same modified donor moiety, chlorination using PPh_3 and CCl_4 was proceeded to facilitate the chloride-terminated chromophore **WJ9**. Hence, three chromophores contained the same donor and acceptor but different π-conjugated electron-bridges. This synthetic strategy contributed to compare their diverse properties caused by different π-conjugated electron-bridges. All chromophores were confirmed by ^{1}HNMR, ^{13}CNMR, element analysis and mass spectrum.

Table 1 Yield of Products **3** and **4**

$POCl_3$: compound 1[a]	Yield of compound **3**	Yield of compound **4**	Overall yield (**3** and **4**)
0.5:1	41%	0	41%
1:1	89%	<1%	89%
2:1	71%	14%	85%
3:1	27%	44%	71%
4:1	16%	36%	52%
6:1	0	28%	28%

[a] Molar Ratio of Precursors

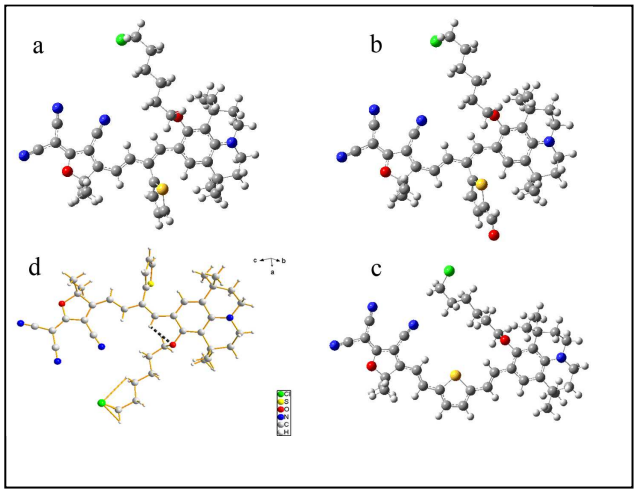

Fig. 1 Optimized structure of chromophores (a: **WJ1**; b: **WJ2**; c: **WJ9**) and crystal conformation of **WJ1** (d)

DFT calculations using Gaussian 03 were carried out at the hybrid B3LYP level employing the split valence 6-31G* basis set.[30] The molecular configuration and geometries were optimized referred to crystal conformation of **WJ1** and analogy chromophore.[31,32] **Fig 1** showed that **WJ1** and **WJ2** contained a shorter divinyl bridge than divinyl-thiophene of **WJ9**. Chromophores with the longer conjugated plane were easier to generate dipole-dipole interactions or aggregation. Moreover, there was no steric hindrance on the conjugated bridge of **WJ9**, while **WJ1** and **WJ2** had the thiophene and formyl-thiophene respectively perpendicular to the electron-bridges playing as the steric hindrance to site-isolate chromophores. Crystal structure of **WJ1** (**Fig. 1d**) confirmed that thiophene was perpendicular to the conjugated plane, playing as the site-isolator to attenuate the dipole-dipole interactions of chromophores.[28] Hence, in geometry analysis of conjugated electron bridges, **WJ1** and **WJ2** might have the more effective steric hindrance than **WJ9** to site-isolate chromophores and to attenuate the dipole-dipole interactions of chromophores. Formyl-thiophene is a larger site-isolator than thiophene, which was supposed that **WJ2** should show better performance in site-isolation than **WJ1**.

2.2 ^{1}HNMR Aanlysis

Site-isolators of thiophene and formyl-thiophene also had the influence on electron distribution and the chemical shift of protons. The two protons on double bond (near TCF) showed the difference of chemical shift Δδ ($\delta_{downfield}$-$\delta_{upfield}$), which was relative to the electron withdrawing ability of acceptor, electron delocalization ability of conjugated electron-bridge and the electron donating ability of donor. **Fig 2** showed the chemical shift of protons on the conjugated plane. Comparing with the divinyl-thiophene based **WJ9**, divinyl based chromophores **WJ1** and **WJ2** revealed totally different chemical shift of protons. The Δδ values of **WJ1**, **WJ2** and **WJ9** are 2.14 ppm, 1.31 ppm and 1.22 ppm. Large Δδ illustrated the extremely non-centrosymmetric structure of electron distribution, easiness of electron delocalization and polarizability of chromophores.[8,33] Electron cloud of electron-rich site-isolators thiophene and formyl-thiophene had the different deshielding effect, which was according to the electron density of site-isolators thiophene and formyl-thiophene. For **WJ2**, the introduction of electron-withdrawing formyl group on the thiophene decreased the electron density of thiophene and the conjugated system. The effects of deshielding and push-pull electron were weakening, showing less Δδ value than that of **WJ1**. Without deshielding effect of site-isolator, **WJ9** showed less Δδ value of 1.22 ppm than **WJ1** and **WJ2**. The electron clouds of site-isolators (thiophene and formyl-thiophene in **WJ1** and **WJ2**) also had the strong deshielding effect to generate the distinct change of chemical shift of singlet proton in donor for all three chromophores. For D-π-A chromophore, if there were well-delocalized electron clouds out of (but quite close to) conjugated plane to distract the antiparallel packing of chromophores, they might contribute to attenuate the formation of dimmer. Hence, this electron-rich site-isolator might be functionalized as the electron-isolator to prevent the antiparallel packing. Thiophene was more electron-delocalized and closer to conjugated plane than formyl-thiophene, so **WJ1** was more effective than **WJ2** in electron-isolation.

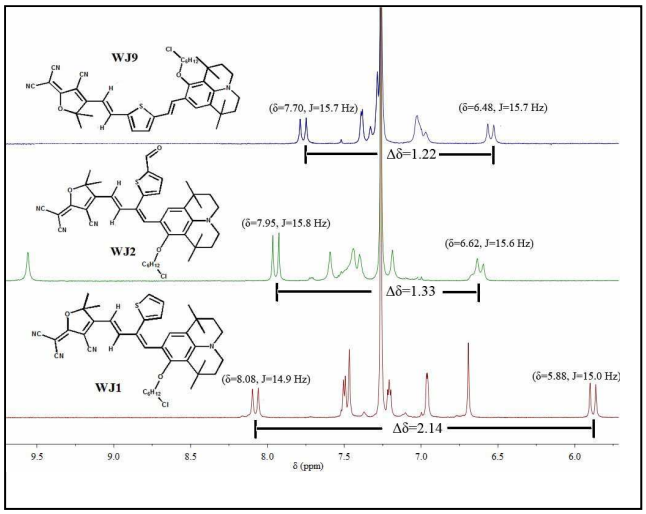

Fig. 2 ^{1}H NMR spectra of chromophores (solvent: $CDCl_3$)

2.3 Photophysical Properties

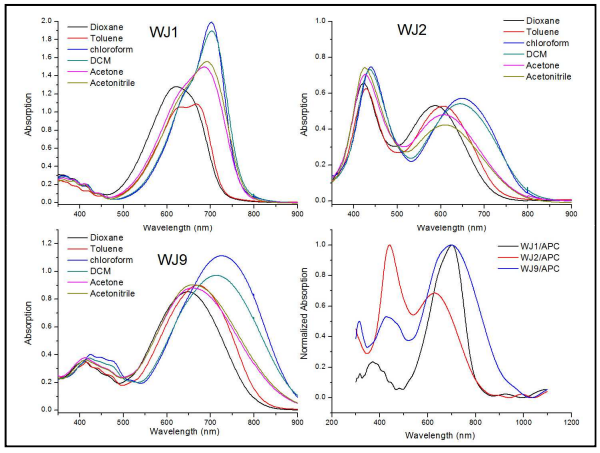

Fig. 3 Solvatochromic behaviors of chromophores **WJ1**, **WJ2** and **WJ9** recorded in different solvents (2×10^{-5} M) of varying dielectric constants and their absorption spectrum of chromophores in guest-host EO polymer

In order to reveal the effect of different conjugated electron-bridges on the electronic structures of chromophores, UV-vis absorption spectra were measured to investigate the intramolecular charge-transfer. As shown in **Fig 3**, all chromophores showed the distinct intramolecular charge-transfer (ICT) absorption band shape and extinction coefficient (ε). From in less polar solvents (dioxane and toluene) to more polar solvents (chloroform, dichloromethane, acetone and acetonitrile), it was observed that **WJ1** had a noticeable spectral shape change showing a dominant low-energy absorption peak and a high-energy shoulder peak. Due to the introduction of electron-withdrawing formyl group, **WJ2** showed two dominant absorption peaks and the high-energy peak had a stronger absorption. **WJ9** had the broadest absorption band with a slight

shoulder peak. In the respect of λ_{max}, WJ9 with longer conjugated bridge showed lower charge-transfer energy, which endowed **WJ9** a larger λ_{max}. Chromophores **B**, **WJ1** and **WJ2** had the similar conjugated bridge, but they showed diverse change of λ_{max} in different solvents. These results could be attributed to the introduction of different electron-isolators. Meantime, it was accompanied by the change of absorption intensity (ε) for all chromophores. **WJ1** showed the most intensified of intramolecular charge-transfer for all chromophores. This result was in coincidence with the conclusion from the ^{1}HNMR analysis that the electron of **WJ1** was more delocalized so that it was easier to have intramolecular charge-transfer, which reflected in the highest absorption intensity. Comparing **WJ1** and **B**, it could be found that introduction of site-isolator effectively enhanced the intensity of intramolecular charge-transfer. While comparing **WJ1** and **WJ2**, it could be found that introduction of electron-withdrawing formyl group had the opposite effect on the absorption intensity.

As shown in **Table 2**, bathochromic shift of λ_{max} from dioxane to chloroform showed that **WJ1** and **WJ9** both exhibited more bathochromic shift of +76 nm. **WJ2** showed less bathochromic shift of +66 nm. To our surprise, chromophore **B** showed the most bathochromic shift from dioxane to chloroform. The most-bathochromically shifted spectra always exhibit the characteristic band shape of a cyanine dye with the most intensified absorbance (ε) and smallest FWHM (full width at half-maximum), suggesting that chromophores **WJ1** and **B**, especially **WJ1** with the most intensified absorption, were easy to be polarized quite close to the cyanine limit in the polar solvents.

Table 2 Photophysical properties of chromophores

	WJ1	WJ2	WJ9	B[e]
λ (ε)$_{dioxane}$	626 (6.39)	587 (2.65)	648 (4.26)	624 (3.51)
λ (ε)$_{toluene}$	667 (5.44)	606 (2.63)	671 (4.50)	636 (4.03)
λ (ε)$_{chloroform}$	702 (9.96)	648 (2.86)	724 (5.56)	711 (7.09)
λ (ε)$_{DCM}$	703 (9.48)	644 (2.71)	713 (4.86)	714 (6.92)
λ (ε)$_{acetone}$	685 (7.49)	607 (2.39)	658 (4.40)	N
λ (ε)$_{acetonitrile}$	692 (7.78)	610 (2.11)	659 (4.51)	699 (5.54)
$\Delta\lambda$[a]	+76	+61	+76	+87
$\Delta\lambda$[b]	-11	-37	-54	-15
FWHM[c]	130	180	202	114
λ film[d]	701	629	698	N

[a] the difference from dioxane to chloroform; [b] the difference from dichloromethane (DCM) to acetonitrile; [c] the full width at half maximum （FWHM）in chloroform; [d] the λ in guest-host EO polycrabonate films containing 25 wt % chromophores; [e] data of chromophore B was selected from reference 29 and N represented not measured; The unit of the maximum absorption wavelength λ, Δλ and FWHM is nanometer (nm); the unit of ε is 10^4 L·mol^{-1}·cm^{-1}; For the solvatochromism of Δλ, + represented the bathochromic shift and - represented the hypochromic shift.

From DCM to acetonitrile, the solvatochromism reversed to a hypsochromic shift, namely inverted solvatochromism.[34] The extent of inverted solvatochromism from DCM to acetonitrile (-11 nm, -30 nm, -54 nm and -15 nm for **WJ1**, **WJ2, WJ9** and **B**, respectively) was quite disordered. For **WJ1**, electron-rich moieties thiophene, which was perpendicular to the conjugated planes, seemed inert to strong polar environment. In other words, the intramolecular electron distribution (electron-isolation) made the intramolecular charge-transfer inert to the neighbor strong polar solvents and chromophores, so that hypsochromic shift of λ_{max} was weaker than other chromophores. Hence, it might be predicted that chromophore with the strongest bathchromism from apolar solvent to polar solvent and the weak hypsochromism from polar solvent to strong polar solvent might be the best candidate to realize the attenuation of dipole-dipole interactions and large macroscopic EO coefficients of materials.

The absorption of chromophores in solid state was also measured. **Table 2** showed the difference of λ_{max} in guest-host EO polymer films and in solution (chloroform) was in accordance with the variation trend of hypsochromic shift. **WJ1** showed the tiny difference of λ_{max} (701 nm in film and 702 nm in chloroform). **WJ2** and **WJ9** had some hypsochromic shifts of 19 nm and 26 nm. There might be intermolecular interactions or other factors to influence the intramolecular charge-transfer in solid films. Anyway, it could be concluded that chromophore **WJ1** in solid state was quite similar to that in solution.

2.4 DFT calculations

Table 3 Energy level (E), dipole moment (μ), polarizability (α), hyperpolarizability (β) and bond-length alternation (BLA) of chromophores[a]

	WJ1	WJ2	WJ9
E_{HOMO} (eV)	-1.967	-1.697	-0.402
E_{LUMO} (eV)	0.0558	0.358	0.938
ΔE (eV)	2.0228	2.055	1.341
μ_x (Debye)	21.10	18.80	18.54
μ_{total} (Debye)	22.63	19.03	22.05
α_{total} (esu)	192.77	196.45	250.35
β_x(10^{-30}esu)	252.98	241.81	825.64
β_{total}(10^{-30}esu)	254.66	246.87	831.20
μβ(10^{-30}esu*D)	5763	4698	18328
BLA (Å)	0.04812	0.04876	0.03761

[a] more details about DFT calculations in Supporting Information.

To obtain further understanding of the conjugated electron-bridge dependent microscopic properties of those chromophores, DFT calculations were carried out and chromophores were rotated into frame such that the *x* axis was aligned with the dipole axis. The relevant theoretical parameters, including HOMO and LUMO levels, dipole moment (μ), polarizability (α), zero-frequency molecular first hyperpolarizability (β) and bond-length alternation (BLA), were displayed in **Table 3**.

Due to different conjugated electron-bridge structure, all chromophores showed the distinct HOMO and LUMO levels. **Fig 4** showed the electron distribution of conjugated plane. It was clear to see that, in HOMO level, electron distributed in the thiophene ring of **WJ1** and lower density of electron in the formyl-thiophene of **WJ2**. Hence, thiophene and formyl-thiophene could respectively be defined as the electron-isolator, by which chromophores were distracted to form antiparallel dimer. In the meantime, the energy gaps (ΔE) of HOMO and LUMO were estimated to be 2.0228, 2.055 and 1.341eV, which was in accordance with the λ_{max} of intramolecular charge-transfer absorption.

Dipole moment (μ) was also calculated for all three chromophores. The μ_{total} of all three chromophores were estimated to be 22.63, 19.03 and 22.05 D, respectively, showing a noticeable change by replacing different conjugated electron-bridge. On the dipolar *x* axis, due to the high electron density on the conjugated plane, **WJ1** showed the largest dipole moment (21.10 D). For **WJ2**, the electron-withdrawing of formyl group

decreased the electron density on *x* axis and the μ_x decreased to 18.80 D, close to 18.54 D of **WJ9**.

In terms of the polarizability, chromophores with large α values were more sensitive to the high voltage electrical field. This property might contribute to the effectively acentric ordering of chromophores in the applied poling electrical field, but it was also likely to induce the dipole-dipole interactions to form the antiparellel dimers. It has been demonstrated that chromophore **WJ9** with the strongest polarizability, was more sensitive to the environment in strong polar solvent and in solid state, which caused the distinct change of λ_{max} in solution and in EO film.

All three chromophores showed a decaying trend in molecular hyperpolarizability as the increasing trend of BLA values from **WJ9** to **WJ1** and **WJ2**. In this regard, we might conclude that divinylthiophene-conjugated chromophore **WJ9** have the much better microscopic nonlinearity than **WJ1** and **WJ2**. But in the case of site-isolation and electron-isolation, **WJ1** and **WJ2** were assumed to have the better performance in the attenuation of dipole-dipole interactions than **WJ9.**

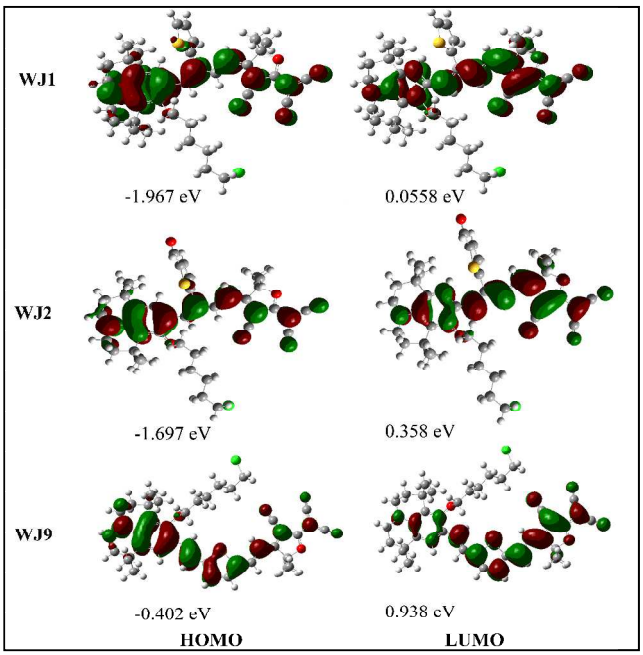

Fig. 4 electron distribution of HOMO and LUMO

2.5 NLO properties

EO coefficient, r_{33}, defining the efficiency of translating molecular microscopic hyperpolarizability into macroscopic EO activities, was described as follows:

$$r_{33} = \left| 2Nf(\omega)\beta \left\langle \cos^3\theta \right\rangle / n^4 \right|$$

where *N* represents the aligned chromophore number density and *f(ω)* denotes the Lorentz-Onsager local field factors. The term $<cos^3\theta>$ is the orientationally averaged acentric order parameter characterizing the degree of noncentrosymmetric alignment of the chromophores in materials and *n* represents the refractive index. Realization of large EO activity for dipolar organic chromophore-containing materials requires the simultaneous optimization of first hyperpolarizability (β), acentric order $<cos^3\theta>$, and number density (*N*).[34] Many sophisticated factors including intramolecular charge-transfer, intermolecular dipole-dipole interactions and molecular shape, as well as the polarizability and hyperpolarizability have the influence on the efficiency of the translation of molecular microscopic nonlinearity into the macroscopic EO coefficients.

As DFT calculations results showed that, **WJ9** possessed better microscopic properties including BLA, $\mu\beta$, and polarizability. In this respect, it was supposed that the EO polymer materials doping **WJ9** have the strongest EO activities. But the EO coefficients of three guest-host doping materials did not fit the variation tendency of microscopic nonlinearity. EO materials of **WJ1/APC**, **WJ2/APC** and **WJ9/APC** containing 20wt% respective chromophores showed r_{33} values of 187 pm/V, 72 pm/V and 37 pm/V, respectively. **WJ9/APC**, containing chromophores **WJ9** with triple μβ values larger than **WJ1** and **WJ2**, showed the lowest r_{33} value. This contrast between microscopic nonlinearity and macroscopic EO coefficients implied that there might be more significant factors to influence the translation of microscopic nonlinearity into macroscopic EO activity.

Indeed, high β value of chromohores is important to determine the macroscopic EO activities. However, hyperpolarizability, no matter it was calculated by DFT or measured by hyper-rayleigh scattering (HRS) in solution, it could not accurately display the microscopic nonlinearity of chromophores in solid EO films. As UV-vis showed, chromophores showed different λ_{max}s and absorption intensity in solution and in films, which was an important factor to determine the hyperpolarizability of chromophores. That meant the hyperpolarizability of chromophore in EO film was no longer as the same as the measured in solution or calculated β value. Hence, this result reminded us to pay more concerns on other factors to improve the macroscopic EO activities.

For the EO materials, each chromophore with the confirmable push-pull structure has the certain intrinsic hyperpolarizability, so the uncertain factors to determine the EO coefficients were the acentric order $<cos^3\theta>$, and number of acentric ordering chromophores (*N*). The acentric order $<cos^3\theta>$ was related to the shape of chromophores, the degree of molecular mobility and steric hindrance. Until now, there was no direct and effective method to characterize the $<cos^3\theta>$ and *N*. But undoubtedly, they significantly determine the r_{33} value. Comparing with the β value, they played the key roles in determining r_{33} values for **WJ1/APC**, **WJ2/APC** and **WJ9/APC**.

In structure analysis, **Scheme 1** showed that there were no steric hindrance group as the site-isolator on the conjugated electron-bridge of chromophores **WJ9** and **B**. Without site-isolator, they were easy to generate the dipole-dipole interaction and form the antiparallel dimmers, so that the true number of acentric ordering chromophores was low in electrical field induced poling. **WJ9/APC** and **B/APC** containing 20wt%chromophores showed r_{33} value of 37 pm/V and 35 pm/V, respectively. For chromophores **WJ1** and **WJ2** containing thiophene and formyl thiophene perpendicular to the conjugated electron-bridge as the site-isolator groups, effective site-isolation distanced the neighbour chromophores. This isolation could attenuate the dipole-dipole interactions and increase the number of oriented

chromophores in electrical field induced poling. Hence, **WJ1/APC** and **WJ2/APC** showed much higher r_{33} value of 187 pm/V and 72 pm/V respectively in 20wt% guest-host EO polymers.

For EO materials **WJ1/APC** and **WJ2/APC,** chromophores **WJ1** and **WJ2** both had the site-isolator to attenuate the dipole-dipole interaction to effectively transfer molecular microscopic nonlinearity to macroscopic EO coefficients of materials. However, different site-isolator group of thiophene and formyl-thiophene indeed generated different molecular properties in ^{1}HNMR analysis and photophysical property analysis. Besides the site-isolation, electron of thiophene and formyl-thiophene was found to have the function of electron-isolation. Thiophene was more electron-delocalized and more electron-rich than formyl-thiophene, so that electron-isolation of thiophene in chromophore **WJ1** was more effective than formyl-thiophene in **WJ2**. This variation of electron-isolation generated more intensified absorption, weaker inverted solvatochromism and more non-centrosymmetric electron distribution of conjugated plane of **WJ1** than **WJ2**. And in EO film, the property of chromophore **WJ1** in solid state was similar to that in solution, indicating that function of electron-isolation could be sufficiently displayed in EO film to distract the antiparallel packing of chromophores. Thus, **WJ1/APC** showed much higher r_{33} value of 187 pm/V than **WJ2/APC** of 72 pm/V in 20wt% guest-host EO polymers.

In terms of the relationship of EO coefficients and chromophore loading density in **Fig 5**, those guest-host EO materials contained the higher chromophore density (>25wt%), **WJ2/APC** and **WJ9/APC** showed the decreased r_{33} values, but **WJ1/APC** showed the ultrahigh r_{33} value of 337 pm/ V as the chromophore density raised to 40wt%. The ultrahigh EO coefficient and rarely high chromophore loading density in guest-host EO materials were the evidences to testify the hypothesis that electron-isolation and site-isolation, especially electron-isolation, might effectively attenuate the intermolecular dipole-dipole interactions of chromophores to achieve the ultrahigh EO coefficients in high chromophore loading density in EO materials.

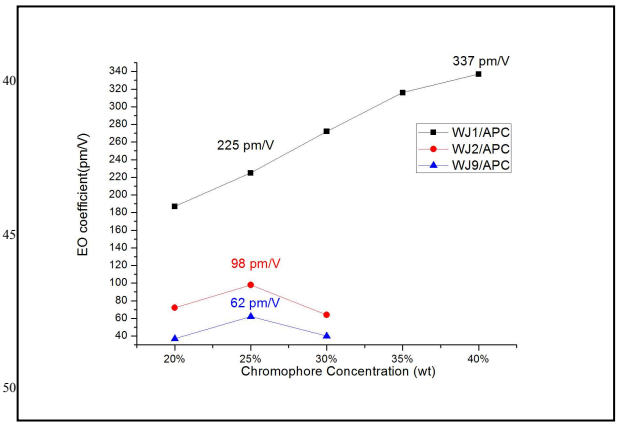

Fig. 5 the relationship of EO coefficient and chromophore concentration

In EO activities, **WJ1/APC** and **WJ2/APC** containing chromophores with site-isolator and electron-isolator showed higher r_{33} values than **WJ9/APC** containing **WJ9** without isolator in conjugated electron-bridge. Moreover, it was indicated that chromophore **WJ1** had more excellent effect on the electron-isolation, so that **WJ1/APC** showed a much higher r_{33} value and it allowed the higher chromophore loading density of 40 wt % to achieve ultrahigh r_{33} value of 337 pm/V.

3. Conclusion

Three chromophores with different conjugated bridge were synthesized through the formylation under different conditions. In acidic formylation, we synthesized the diene-conjugated chromophores **WJ1** and **WJ2** containing thiophene and formyl-thiophene respectively perpendicular to the conjugated planes. As the site-isolators, steric hindrances of thiophene and formyl-thiophene were more effective to attenuate the dipole-dipole interactions for chromophores **WJ1** and **WJ2** than divinyl-thiophene conjugated chromophore **WJ9**. More intriguingly, the site-isolators had significant influence on the photophysical properties, intramolecular charge-transfer, and electron distribution and theoretically calculated molecular microscopic properties. It was confirmed that site-isolators also played as the electron-isolators, which greatly contributed to generate the weak inverted solvatochromism in strong polar solvents and made the photophysical properties of chromophores in EO films as excellent as in solution. In EO activities, it showed that site-isolation and electron-isolation were the more important factors than molecular microscopic hyperpolarizability to influence the EO coefficients of materials. Moreover, comparing the EO materials **WJ1/APC** and **WJ2/APC**, it was indicated that **WJ1** containing thiophene as a more effective electron-isolator had the most powerful effect to attenuate the dipole-dipole interactions of chromophores in EO films. **WJ1/APC** showed the ultrahigh r_{33} value at high chromophore density. Those comparisons inspired us that introduction of electron-delocalized moiety into the chromophore, functionalized as the electron-isolation and site-isolation, might be an effective path to attenuate the dipole-dipole interactions of chromophores and further to efficiently translate the microscopic nonlinearity into macroscopic EO coefficients.

4. Acknowledgment

We are grateful to the Directional Program of the Chinese Academy of Sciences (KJCX2.YW.H02), Innovation Fund of the Chinese Academy of Sciences (CXJJ-11-M035) and the National Natural Science Foundation of China (No.61101054) for financial support.

5. Notes and references

[a] *School of Communication and Information Engineering, University of Electronic Science and Technology of China, Chengdu, China. E-mail: jieyunwu@uestc.edu.cn*

[b] *Key Laboratory of Photochemical Conversion and Optoelectronic Materials, Technique Institute of Physics and Chemistry, Chinese Academy of Sciences, Beijing, China. E-mail: boshuhui@mail.ipc.ac.cn*

† Electronic Supplementary Information (ESI) available: [details of experiment and DFT calculations]. See DOI: 10.1039/b000000x/

‡ Footnotes should appear here. These might include comments relevant to but not central to the matter under discussion, limited experimental and spectral data, and crystallographic data.

Reference

(1) Sullivan, P. A.; Dalton, L. R. *Accounts Chem Res* **2010**, *43*, 10-18.

(2) Davies, J. A.; Elangovan, A.; Sullivan, P. A.; Olbricht, B. C.; Bale, D. H.; Ewy, T. R.; Isborn, C. M.; Eichinger, B. E.; Robinson, B. H.; Reid, P. J.; Li, X.; Dalton, L. R. *J Am Chem Soc* **2008**, *130*, 10565-10575.
(3) Hammond, S. R.; Sinness, J.; Dubbury, S.; Firestone, K. A.; Benedict, J. B.; Wawrzak, Z.; Clot, O.; Reid, P. J.; Dalton, L. R. *J Mater Chem* **2012**, *22*, 6752.
(4) Pereverzev, Y. V.; Gunnerson, K. N.; Prezhdo, O. V.; Sullivan, P. A.; Liao, Y.; Olbricht, B. C.; Akelaitis, A. J. P.; Jen, A. K. Y.; Dalton, L. R. *J Phys Chem C* **2008**, *112*, 4355-4363.
(5) Jen, A.; Zhou, X. H.; Davies, J.; Huang, S.; Luo, J. D.; Shi, Z. W.; Polishak, B.; Cheng, Y. J.; Kim, T. D.; Johnson, L. *J Mater Chem* **2011**, *21*, 4437-4444.
(6) Shi, Y. Q.; Zhang, C.; Zhang, H.; Bechtel, J. H.; Dalton, L. R.; Robinson, B. H.; Steier, W. H. *Science* **2000**, *288*, 119-122.
(7) Dalton, L. In *Adv Polym Sci*; Springer-Verlag Berlin: Berlin, 2002; Vol. 158; pp 1-86.
(8) Hammond, S. R.; Clot, O.; Firestone, K. A.; Bale, D. H.; Lao, D.; Haller, M.; Phelan, G. D.; Carlson, B.; Jen, A. K. Y.; Reid, P. J.; Dalton, L. R. *Chem Mater* **2008**, *20*, 3425-3434.
(9) Luo, J.; Huang, S.; Shi, Z.; Polishak, B. M.; Zhou, X.-H.; Jen, A. K. Y. *Chem Mater* **2011**, *23*, 544-553.
(10) Sullivan, P. A.; Akelaitis, A. J. P.; Lee, S. K.; McGrew, G.; Lee, S. K.; Choi, D. H.; Dalton, L. R. *Chem Mater* **2006**, *18*, 344-351.
(11) Kim, T. D.; Luo, J. D.; Cheng, Y. J.; Shi, Z. W.; Hau, S.; Jang, S. H.; Zhou, X. H.; Tian, Y.; Polishak, B.; Huang, S.; Ma, H.; Dalton, L. R.; Jen, A. K. Y. *J Phys Chem C* **2008**, *112*, 8091-8098.
(12) Li, Z.; Li, Q.; Qin, J. *Polymer Chemistry* **2011**, *2*, 2723.
(13) Z. Li, W. W., C. Ye, J. Qin and Z. Li, Polym. Chem., 2010, 1, 78.
(14) Wu, J.; Wilson, B. A.; Smith Jr, D. W.; Nielsen, S. O. *Journal of Materials Chemistry C* **2014**, *2*, 2591.
(15) Wu, W.; Huang, Q.; Xu, G.; Wang, C.; Ye, C.; Qin, J.; Li, Z. *Journal of Materials Chemistry C* **2013**, *1*, 3226.
(16) Wu, W.; Wang, C.; Tang, R.; Fu, Y.; Ye, C.; Qin, J.; Li, Z. *Journal of Materials Chemistry C* **2013**, *1*, 717.
(17) Wu W, Q. J., Li Z. Polymer, 2013, 54: 4351.
(18) Wu, W.; Huang, L.; Song, C.; Yu, G.; Ye, C.; Liu, Y.; Qin, J.; Li, Q.; Li, Z. *Chemical Science* **2012**, *3*, 1256.
(19) Wu, W.; Huang, L.; Xiao, L.; Huang, Q.; Tang, R.; Ye, C.; Qin, J.; Li, Z. *RSC Advances* **2012**, *2*, 6520.
(20) Wu, W.; Yu, G.; Liu, Y.; Ye, C.; Qin, J.; Li, Z. *Chemistry* **2013**, *19*, 630-41.
(21) Wu, W.; Huang, Q.; Qiu, G.; Ye, C.; Qin, J.; Li, Z. *J Mater Chem* **2012**, *22*, 18486.
(22) Li, Z.; Wu, W.; Li, Q.; Yu, G.; Xiao, L.; Liu, Y.; Ye, C.; Qin, J. *Angew Chem Int Ed Engl* **2010**, *49*, 2763-7.
(23) Wu, W; Z, Z.; Qiu, G.; Ye, C.; Qin, J.; Li, Z. J Polym Sci Part A Polym Chem; 2012;50:5124.
(24) Wu, W.; Y, C.; Qin, J.; Li Z. Polym Chem 2013;4:2361.
(25) Li, Z.; W, W.; Ye, C.; Qin, J.; Li, Z. Polymer 2012;53:153.
(26) Li, Z.; Y, G; Dong, S.; Wu, W.; Liu, Y.; Ye, C.; et al. Polymer 2009;50:2806.
(27) Zeng, Q.; L, Z.; Li, Z.; Ye, C.; Qin, J.; Tang, B. Macromolecules 2007;40:5634.
(28) Wu, J.; Bo, S.; Liu, J.; Zhou, T.; Xiao, H.; Qiu, L.; Zhen, Z.; Liu, X. *Chem Commun* **2012**, *48*, 9637-9.
(29) Zhang, M.; Deng, G.; Zhang, A.; Xu, H.; Huang, H.;Peng, C.; Bo, S.; Liu, J.; Liu, X.; Zhen, Z.; Qiu, L. RSC Adv, 2014, 4, 33312-33318
(30) JR, M. J., Vreven T, Kudin KN, Burant JC, Millam JM, Iyengar SS, Tomasi J, Barone V, Mennucci B, Cossi M, Scalmani G, Rega N, Petersson GA, Nakatsuji H, Hada M, Ehara M, Toyota K, Fukuda R, Hasegawa J, Ishida M, Nakajima T, Honda Y, Kitao O, Nakai H, Klene M, Li X, Knox JE, Hratchian HP, Cross JB, Adamo C, Jaramillo J, Gomperts R, Stratmann RE, Yazyev O, Austin AJ, Cammi R, Pomelli C, Ochterski JW, Ayala PY, Morokuma K, Voth GA, Salvador P, Dannenberg JJ, Zakrzewski VG, Dapprich S, Daniels AD, Strain M C, Farkas O, Malick D K, Rabuck A D, Raghavachari K, Foresman J B, Ortiz J V, Cui Q, Baboul A G, Clifford S, Cioslowski J,Stefanov B B, Liu G, Liashenko A, Piskorz P, Ko-maromi I, Martin RL, Fox DJ, Keith T, Al-Laham MA, Peng CY, Nanayakkara A, Challacombe M, Gill PMW, Johnson B, Chen W, Wong MW, Gonzalez C, Pople JA. *Gaussian 03, Gaussian, Inc., Pittsburgh, PA, 2003*.
(31) Wu, J.; Liu, J.; Zhou, T.; Bo, S.; Qiu, L.; Zhen, Z.; Liu, X. *RSC Advances* **2012**, *2*, 1416.
(32) Wu, J.; Peng, C.; Xiao, H.; Bo, S.; Qiu, L.; Zhen, Z.; Liu, X. *Dyes Pigments* **2014**, *104*, 15-23.
(33) Würthner, F.; Archetti, G.; Schmidt, R.; Kuball, H.-G. *Angewandte Chemie International Edition* **2008**, *47*, 4529-4532.
(34) Dalton, L. R.; Lao, D.; Olbricht, B. C.; Benight, S.; Bale, D. H.; Davies, J. A.; Ewy, T.; Hammond, S. R.; Sullivan, P. A. *Opt Mater* **2010**, *32*, 658-668.